ACS APPLIED MATERIALS & INTERFACES

Research Article

www.acsami.org

Autonomic Self-Healing in Epoxidized Natural Rubber

Md Arifur Rahman,*[,†] Luciana Sartore,[†] Fabio Bignotti,[†] and Luca Di Landro[‡]

[†]Department of Mechanical and Industrial Engineering, University of Brescia, Via Valotti 9, 25123 Brescia, Italy

[‡]Department of Aerospace Science & Technology, Polytechnic of Milan, via La Masa 34, 20156 Milano, Italy

ABSTRACT: The development of polymers that can repair damage autonomously would be useful to improve the lifetime of polymeric materials. To date, limited attention has been dedicated to developing elastomers with autonomic self-healing ability, which can recover damages without need for an external or internal source of healing agents. This work investigates the self-healing behavior of epoxidized natural rubber (ENR) with two different epoxidation levels (25 and 50 mol % epoxidation) and of the corresponding unfunctionalized rubber, *cis*-1,4-polyisoprene (PISP). A self-adhesion assisted self-healing behavior was revealed by T-peel tests on slightly vulcanized rubbers. A higher epoxidation level was found to enhance self-healing. Self-healing of rubbers following ballistic damages was also investigated. A pressurized air flow test setup was used to evaluate the self-healing of ballistic damages in rubbers. Microscope (OM, SEM, and TEM) analyses were carried out to provide further evidence of healing in the impact zones. Self-healing of ballistic damages was observed only in ENR with 50 mol % epoxidation and it was found to be influenced significantly by the cross-link density. Finally, self-healing of ballistic damages was also observed in ENR50/PISP blends only when the content of the healing component (i.e., ENR50) was at least 25 wt %. From an analysis of the results, it was concluded that a synergistic effect between interdiffusion and interaction among polar groups leads to self-healing in ENR.

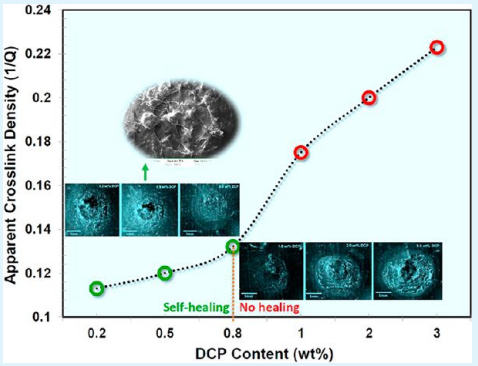

KEYWORDS: *self-healing elastomer, self-adhesion, epoxidized natural rubber, ballistic damage, rubber blends*

INTRODUCTION

Recovery of damages in polymers and composites has been a fundamental concern in materials science and technology for a long time. In the last two decades, intensive research works have been carried out to engineer materials with self-healing abilities.[1] Most of the self-healing materials require external energy such as heat or light for the healing,[2−4] a few systems require healing agents[5,6] for the damage healing of the matrix polymer, and some systems require change in internal pH following a corrosion event (that leads to either mechanical or chemical rupture of multilayer polymer film), which triggers the release of corrosion inhibitor and thus terminates the corrosion process in metal surface or prolongs the corrosion protection.[7−9]

Although large interest has been devoted to stiff materials and composites, very few approaches have been reported on the investigation of self-healing elastomers.[10−16] Such materials can have a wide range of applications such as sealing joints, impact protection, insulation and shock-absorbing layers, anticorrosion coatings for metals, and as adhesives or paints.[17−20] For most self-healing elastomers, external stimuli are required to achieve healing. For example, noncovalent supramolecular linkages have been introduced into a polymer that can heal upon heating.[10,11] However, for many applications, autonomous healing of the rubber, without any external stimuli, is desirable. Cordier et al.[12] developed a dynamic supramolecular approach to synthesizing a self-healing rubber with multivalent hydrogen bonds; these are individually weak but collectively can form a network at room temperature with remarkable load-bearing capacity,[13] allowing autonomic healing of the damage. In a recent work, they explored the self-healing behavior of a supramolecular rubber by tack-like experiments and they showed that self-adhesive strength of rubber surfaces could be enhanced by the damage processes.[14] Chen et al.[15] developed a thermoplastic elastomer with a multiphase supramolecular design containing polystyrene backbone as the hard phase and polyacrylate amide as the soft phase; they proposed that self-healing takes place because of reversible hydrogen bonding in the soft matrix. Recently, Zheng et al.[16] reported heat-induced self-healing behavior of newly synthesized cross-linked poly(dimethyl siloxane) elastomer (this elastomer has also been considered as "living polymer network"), where the healing mechanism is due to the presence of reactive end groups that can react with network chains upon heating; such reaction restores the cross-links in the network and catalyzes the anionic equilibration with the network.

Although many efforts[11−16] have been committed to synthesizing self-healing elastomers based on supramolecular chemistry, limited attention has been drawn to identifying self-healing of conventionally synthesized rubbers. In particular, no

Received: December 7, 2012
Accepted: February 4, 2013
Published: February 4, 2013

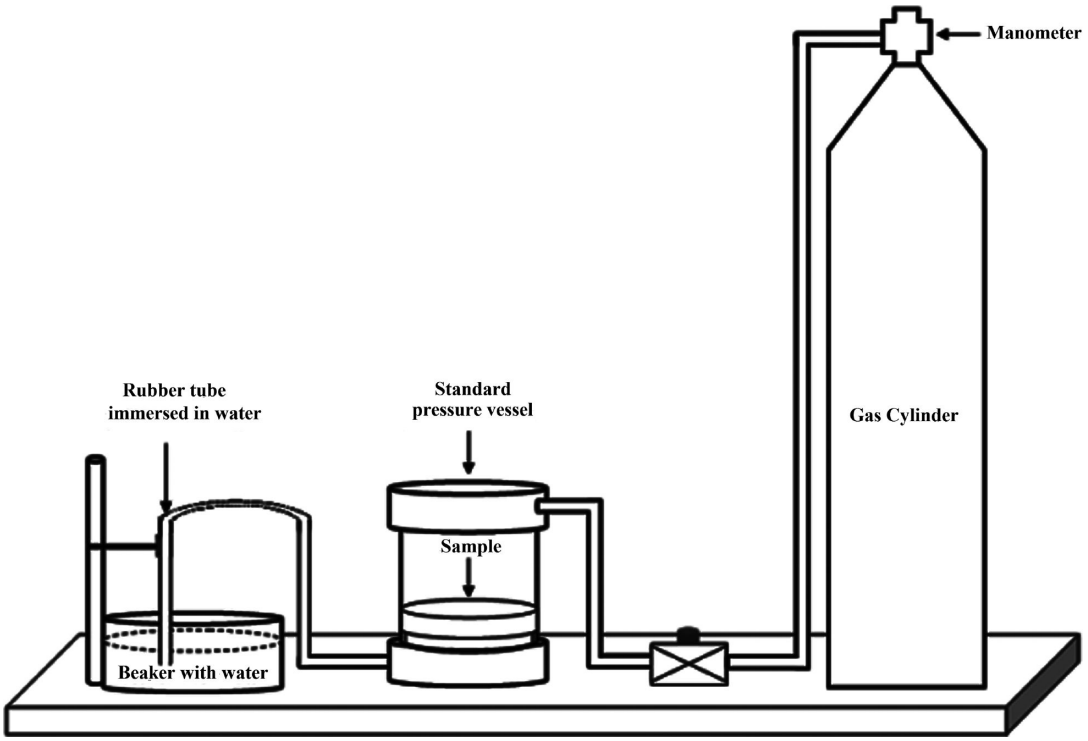

Figure 1. Experimental setup for the evaluation of self-healing by the pressurized air flow test.

literature can be found in which the damage healing of epoxidized natural rubber (ENR) is examined.

This paper investigates the autonomic healing response of epoxidized natural rubber in ballistic and slow, self-adhesion tests. ENR was first synthesized in 1922[21] but an industrially viable synthetic route was developed only in the mid-1960s.[22,23] The chemical modification of ENR is usually done commercially by in situ epoxidation of natural rubber (NR) latex using hydrogen peroxide and formic acid.[24] Under carefully controlled conditions, NR latex can be epoxidized to over 75 mol % without the formation of secondary ring opened structures.[24] It is well-known that the epoxidation reactions are stereospecific[25] and thus ENR is a *cis*-1,4-polyisoprene with epoxide groups randomly distributed along the polymer backbone. Most of the studies on ENR are confined to ENR25 and ENR50 (25 and 50 mol % epoxidation, respectively) which are the commercially available grades. Because of the polar nature of the oxirane groups, epoxidized NR exhibits various useful properties, e.g., low gas permeability,[26] oil resistance,[27,28] as well as enhanced compatibility with polymers bearing polar groups like polyamide[28] or PVC.[29] In addition, ENR, which is able to undergo strain crystallization, possesses high tensile properties and has good resistance to crack propagation up to 50 mol % epoxidation.[30] In previous articles[31,32] concerning ionomer-based blends with ENRs, we gained some indications about the ballistic self-repairing ability of ENR50 but no systematic work was done on the self-healing behavior of epoxidized natural rubber, especially regarding the effect of epoxidation level.

In this research work, ENR with two different epoxidation levels (25 and 50 mol % epoxidation) and the corresponding unfunctionalized rubber, cis-1,4-polyisoprene (PISP) were studied to understand the role of functionality on the self-healing in rubbers. The effect of cross-link density on the self-healing of ENR was also investigated. Moreover, blends of ENR50 with PISP were prepared to investigate the role of ENR50 content on their damage healing efficiency. Self-healing of these rubbers was studied in two different test conditions/damage modes: T-peel tests and ballistic tests. The healing behavior of rubbers following self-adhesion was investigated by T-peel tests. The ballistic self-healing efficiency was determined on the basis of air tightness tests at different pressure levels after bullet impact punctures. Morphological observations by optical microscopy and SEM of the impact zones, as well as TEM analysis of the blends, were carried out to provide further evidence of healing in the damage zones.

EXPERIMENTAL SECTION

Materials. Epoxidized natural rubbers having 25 and 50 mol % epoxidation levels with trade names of Epoxyprene 25 and Epoxyprene 50, respectively, were purchased from SAN-THAP International Company Ltd., Thailand. Molecular weights of 6.8×10^4 and 3.9×10^4 g/mol were reported by the manufacturer for pure ENR25 and ENR50, respectively. *cis*-1,4-Polyisoprene (97% cis 1,4) was purchased from Sigma-Aldrich. The intrinsic viscosity $[\eta]$ of *cis*-1,4-polyisoprene rubber, measured in toluene at 30 °C using an Ubbelohde viscometer, was 670 mL g^{-1}. From the Mark–Houwink relationship, $[\eta] = k\bar{M}_v^a$, a viscosity-average molecular mass $\bar{M}_v$ of 2.3×10^6 g mol^{-1} was calculated using values of $k = 8.51\times 10^{-3}$ mL g^{-1} and $a = 0.77$.[33]

Dicumyl peroxide (DCP), used as a cross-linking agent for rubbers, was also purchased from Sigma-Aldrich.

Sample Preparation. Samples of ENR25, ENR50, and PISP were prepared by vulcanizing with DCP. At first the pure rubber was melt mixed with DCP (0.5 wt %) in a twin-screw Brabender (Plastograph, Germany) at 100 °C with a screw speed of 80 rpm. The melt mixed samples were then vulcanized by compression molding at 160 °C for 13 min to produce square plates ($100\times 100\times 2$ mm^3).

ENR50 samples with additional cross-link densities were prepared by following the above-mentioned procedure but using different DCP contents (0.2, 0.5, 0.8, 1, 2, and 3 wt %).

Blends of ENR50 and PISP having 15, 25, and 50 wt % PISP content were also prepared by melt-mixing in the Brabender at 100 °C

with 0.5 wt % DCP. The melt mixed samples were then compression molded at 160 °C for 13 min to produce square plates.

T-Peel Test. Strips 100 mm long and 20 mm wide were cut from the molded sheets. Two strips of rubbers having 2 mm thickness were brought into contact under a controlled pressure of 245 Pa. The length of the bonded and unbounded rubber strips in each sample were 40 and 60 mm, respectively. A flat weight was used to provide the pressure for a known period of time (5 min) at room temperature. To understand the effect of temperature and contact time on the peel strength, we treated all samples at two different temperatures (at 25 °C and at 60 °C) for different contact times (0.5, 3, 24, and 72 h) with no pressure applied. For all samples, we carried out T-peel tests at 25 °C.

The ENR strips were peeled from each other using a T-peel geometry in an Instron Testing machine (Instron 3366 Dynamometer) at a constant cross-head speed of 10 mm/min. The peel strength, P, was calculated from the average peel force, F, using the relation

$$P = F/w$$

Where w is the width of the strips.

Ballistic Tests and Evaluation of Self-Healing. Ballistic puncture tests were carried out on all vulcanized rubber samples of square geometry (100 × 100 × 2 mm^3 plates) at room temperature. The tests were performed in a local police station shooting facility with 9 × 21 mm^2 bullets with a speed range from 360 to 380 m/s. To check the occurrence of healing at the impact zones, we devised a setup to have quantitative estimation of healing efficiency in different samples. The device setup allows to give evidence of hole closure at the impact zones by applying a pressurized air flow; it consists of an ultrafiltration standardized pressure vessel (Amicon, Germany) equipped with controllable fluid flow by a rubber tube attached to the manometer of a nitrogen cylinder. Figure 1 shows an image of setup for the whole procedure. Circular plates cut from punctured samples were placed inside the pressure vessel and subjected to defined pressure differences; the sealing of the specimens, to avoid possible gas leaks out of the pressure vessel, was checked before tests by immersion in a water containing vessel. During tests, an outward rubber tube was kept inside a beaker containing water. The circular plate of samples inside the pressure vessel was exposed to a pressure differences ranging from 0.5 to 2 bar for specified period of times (Table 1). The failure of healing was identified if water bubbles were observed inside the beaker within 10 min, at the initial pressure difference of 0.5 bar. The healing efficiency of samples was evaluated from the absence of water bubbles at increasing levels of pressure differences (i.e., 0.5 to 2.0 bar). In addition, all specimens were also observed by optical stereomicroscope both in the bullet entrance and exit sides at 10× to 100× magnifications to confirm hole closure.

FTIR Analysis. The chemical structures of films were investigated using Fourier transform infrared analysis (FTIR-ATR (JASCO-300E)). The specimens were dried in a vacuum desiccator with P_2O_5 for 24 h before the experiment. The spectra were recorded between 4000 and 650 cm^{-1} (256 scans, resolution 2 cm^{-1}) using a Jasco FTIR 5300 spectrometer equipped with a PIKE MIRacle diamond ATR accessory.

Cross-Link Density Measurements. An index of cross-link density was determined by equilibrium swelling tests. Swelling experiments were carried out on vulcanized samples by immersing the samples in toluene at room temperature for 48 h in order to achieve the equilibrium swelling condition. The swelling ratio (Q) was calculated as $Q = (W_s - W_u)/W_u$, where W_s and W_u are the weights of the swollen and unswollen samples. The reciprocal swelling ratio ($1/Q$) at equilibrium was used as the indication of the apparent cross-link density.[34]

Scanning Electron Microscopy (SEM). Scanning electron microscopic (SEM) analyses were carried out on the damaged surfaces of the specimens using a scanning electron microscope (LEO EVO 40). Samples were mounted with carbon tape on aluminum stubs and then sputter-coated with gold to make them conductive prior to SEM observation.

Transmission Electron Microscopy (TEM). The samples were microtomed at −80 °C using a Leica EM UC7 ultramicrotome with a Leica EM FC7 cryo chamber attachment. The sections were observed unstained in a transmission electron microscope (TEM) FEI CM120.

Table 1. Results of Pressurized Air Flow Tests

	pressure drop/failure [(+)/(−) ve][a] at different pressure differences[b] (bar)			
materials (wt % DCP)	0.5	0.8	1.0	2.0
PISP (0.5 DCP)	(+)ve			
ENR25 (0.5 DCP)	(+)ve			
ENR50 (0.2 DCP)	(−)ve	(−)ve	(−)ve	(−)ve
ENR50 (0.5 DCP)	(−)ve	(−)ve	(−)ve	(−)ve
ENR50 (0.8 DCP)	(−)ve	(−)ve	(−)ve	(−)ve
ENR50 (1.0 DCP)	(+)ve			
ENR50 (2.0 DCP)	(+)ve			
ENR50 (3.0 DCP)	(+)ve			
ENR50/PISP blends (wt % PISP)				
15	(−)ve	(−)ve	(−)ve	(−)ve
25	(−)ve	(+)ve		
50	(+)ve			

[a]Pressure drop is ((+)ve) when impact zone cannot maintain pressure at the impact zone for at least 10 min because of the incomplete hole closure and ((−)ve) when impact zone maintained pressure for a specified period of time. [b]These pressure levels at the impact zones were maintained for 10 mints.

RESULTS AND DISCUSSION

Self-Healing Assisted by Self-Adhesion in Rubbers. Peel or adhesion testing usually measures the adhesive or bond strength between two materials. T-peel tests on the same rubber samples, where the materials are pulled axially away from each other, can give indication about the ability of two adjacent surfaces of the same substance to give a sturdy connection preventing their separation at the place of contact. Such a phenomenon is usually ascribed to self-adhesion of two intimate surfaces of the same material because of the strong interdiffusion process at the interface.[35]

Although different types of physical or chemical interaction between two similar or dissimilar material surfaces can be defined as the adhesion forces, the self-adhesion behavior of flexible materials should actually be considered as cohesion where interactions take places between similar substances. In the self-healing process, two surfaces that were initially separated are able to reach intimate contact and restore the structural integrity of the system; considering this reason, we have investigated the self-healing of rubbers by measuring their peel strength in T-peel mode.

It should be noted that in the tested materials this behavior should not be ascribed to tackiness, i.e., the property of an adhesive that enables it to instantly form a bond when brought into contact with another surface.[36]

The T-peel tests were carried out on slightly vulcanized (0.5 wt % DCP) rubbers (i.e., PISP, ENR25, and ENR50). Since the duration of contact and temperature play an important role on the adhesion of rubbers, this test was performed on samples treated at two different temperatures (25 and 60 °C) for different periods of time (0.5 to 72 h).

Panels a and b in Figure 2 show the peel strength of PISP, ENR25 and ENR50 rubber as a function of contact time and temperatures. It can be noticed that at 25 °C, the peel strength clearly increases (Figure 2a) with increasing contact time for ENR25 and ENR50 samples, whereas only a slight increase can

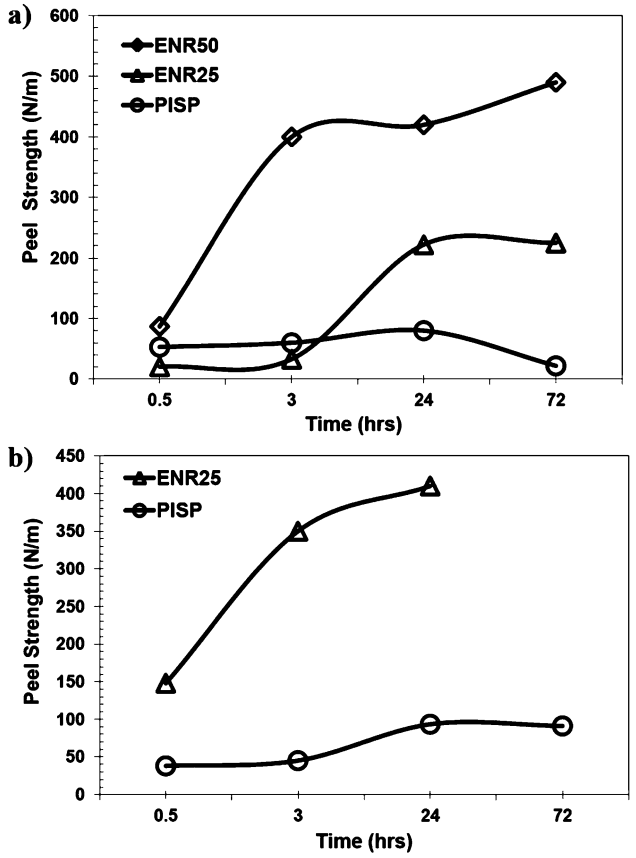

Figure 2. Results of T-peel tests showing the peel strength of PISP, ENR25, and ENR50 (vulcanized with 0.5 wt % DCP) at different contact times for the samples treated at (a) 25 and (b) 60 °C.

be observed for PISP (Figure 2a). However, the peel strength is always higher in ENR50, whereas the lowest is observed in PISP and ENR25 shows intermediate values at least at long contact times. Higher peel strength values were found for the samples treated at 60 °C. It can be noticed that data for all ENR50 and ENR25 at 72 h of contact are not shown in Figure 2b. In fact, for these samples, full stretching of peel arms was reached with increasing load, but no separation at the joints. Correspondingly, the curves recorded did not show the typical feature of a peel curve.

Panels a and b in Figure 3 show, as example, the peel records of ENR25 and ENR50 samples treated at 60 °C for 0.5 h. It can be noticed that a typical peel curve was obtained for ENR25 (Figure 3a) but not for ENR50 (Figure 3b). Such behavior, which was observed for all ENR50 samples treated at 60 °C for different contact times, can be ascribed to a complete cohesion of two surfaces at the interface. In addition, all the peel records for samples treated at 60 °C are comparable to the tensile behavior of the virgin sample. Figure 3 (c) shows the typical load vs extension curve obtained for ENR50 (0.5 DCP) in tensile mode. It can be noticed that the bond strength of joints for ENR50 sample (treated at 60 °C for 0.5 h) in T-peel mode recovers almost 70% of virgin strength as seen in Figure 3c. Thus, the T-peel test results might be explained by assuming that a higher temperature promotes interdiffusion of polymer chains, whereas a higher level of epoxidation promotes stronger interactions at the interface and thus leads to the self-healing of adjoining surfaces of ENR50.

It can be observed that all rubbers were vulcanized with the same amount of DCP (0.5%). Notwithstanding the different initial molecular weight of ENR and PISP, little difference should thus be expected in the average molecular weight of chain segments between cross-links (M_x). Assuming that any DCP molecules produces two reactive radicals an average M_x value of 27 000 Da can be estimated for 0.5% DCP; somewhat higher M_x values are obtained considering a cross-linking efficiency of DCP lower than 1.[37] However, such value is well comparable to the entanglement molecular (M_e) of about 7000 Da or to the critical mol wt (M_c) of 15 000 Da reported for PISP,[38] which are related to the average distance between interchain entanglements. As a consequence, it is expected that only few intermolecular entanglements may be formed between the joining surfaces even in equilibrium contact conditions. These considerations support the fact that for the considered materials, simple interdiffusion is not sufficient for an efficient self-adhesion, but intermolecular forces, as in ENR50 are necessary to restore full joint strength. Because the intermolecular interaction is governed by the presence of polar groups in ENR, FTIR analysis can be useful to have the compositional structure of ENR.

Figure 4 shows the FTIR spectra of pure PISP, ENR25, and ENR50. The spectra of both ENR25 and ENR50 show the presence of epoxy group at 873 and 1249 cm^{-1}. It is important to notice a broad and intense peak present in the spectrum of ENR50 in the region of 3200−3450 cm^{-1}, which is associated with the presence of hydroxyl group. In addition, another small peak in the region of 1728 cm^{-1} indicates the presence of C═O group in ENR50. However, both the OH and C═O groups are absent in the spectra of pure ENR25 and PISP. Moreover, the presence of cyclic ether at 1070 cm^{-1} can be observed in both ENR25 and ENR50 but the intensity is higher in ENR50. Several articles reported that during the synthesis of ENR some epoxide ring-opened products (i.e., OH, C═O, or cyclic ethers) can form because of the low pH, high temperature, or longer synthesis time.[18,39,40] As a consequence, a higher epoxidation level increases the concentration of ring-opened byproducts and ultimately the polar group content in ENR. Thus, from the FTIR analysis, it can be inferred that intermolecular hydrogen bonding takes place at the interface of rubber joints. This explains why ENR50, which has a higher epoxidation level, exhibited a higher peel strength.

Self-Healing of Ballistic Damages in Rubbers. *Evaluation of Self-Healing in Rubbers with Different Epoxy-Functionalization Levels.* The ballistic damage initiated self-healing behavior was investigated in epoxidized natural rubbers with 25 mol % (ENR25) and 50 mol % (ENR50) epoxidation levels and also in unfunctionalized PISP. Initially, ballistic tests were performed on rubber samples slightly vulcanized (with 0.5 wt % DCP), then pressurized air flow tests were carried out to evaluate the air tightness of the punctured zone in the samples. Table 1 summarizes the results of the pressurized air flow tests, which revealed complete hole closure in ENR50 sample whereas a pressure drop at the impact zones of ENR25 and PISP indicated the presence of holes in the impact zones. Figure 5a−c shows the optical images of the impact zones in slightly vulcanized rubber samples after the ballistic tests with 9 × 21 mm^2 bullet. Although in all cases puncture area is small if compared to bullet diameter, clear holes can be observed in the impact zones of PISP and ENR25 samples, whereas complete closure can be observed in ENR50 sample (Figure 5a). It is also important to mention here that some burnt part of the sample

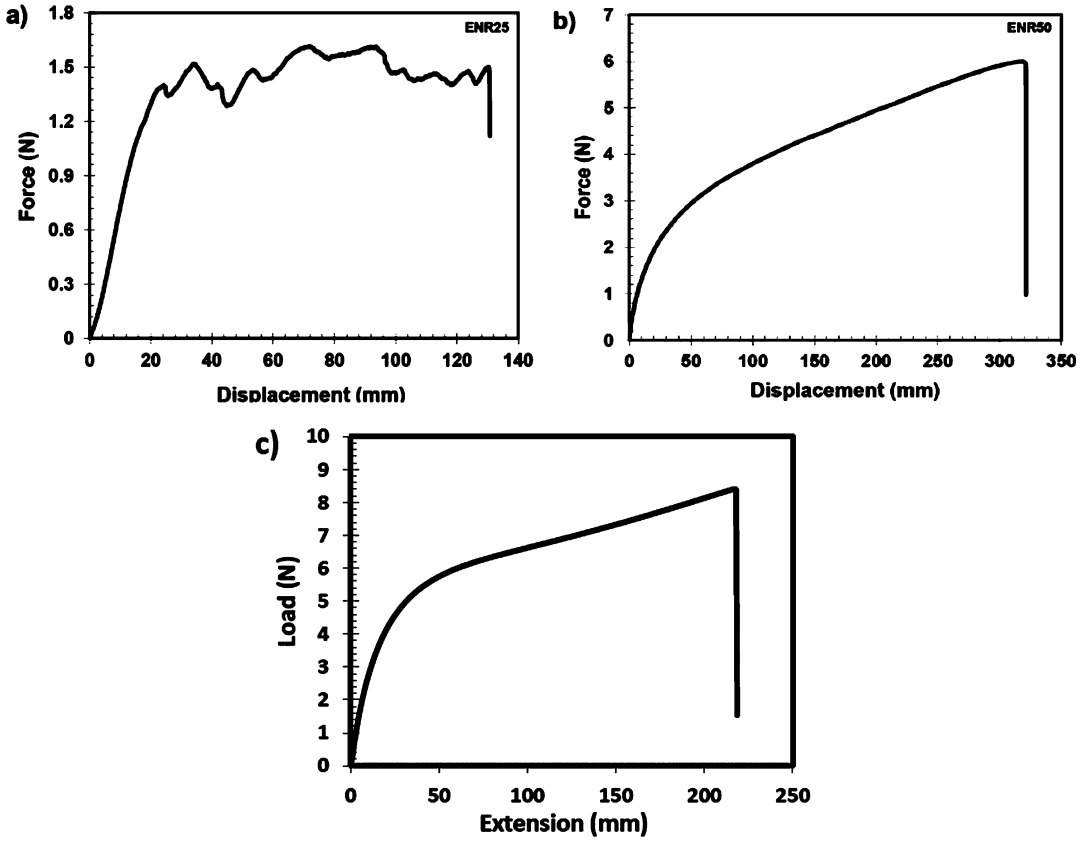

Figure 3. Peel records of samples treated at 60 °C for a contact time of 0.5 h; (a) ENR25 and (b) ENR50; and (c) typical load vs extension curve for ENR50 (0.5 DCP) sample obtained in tensile mode.

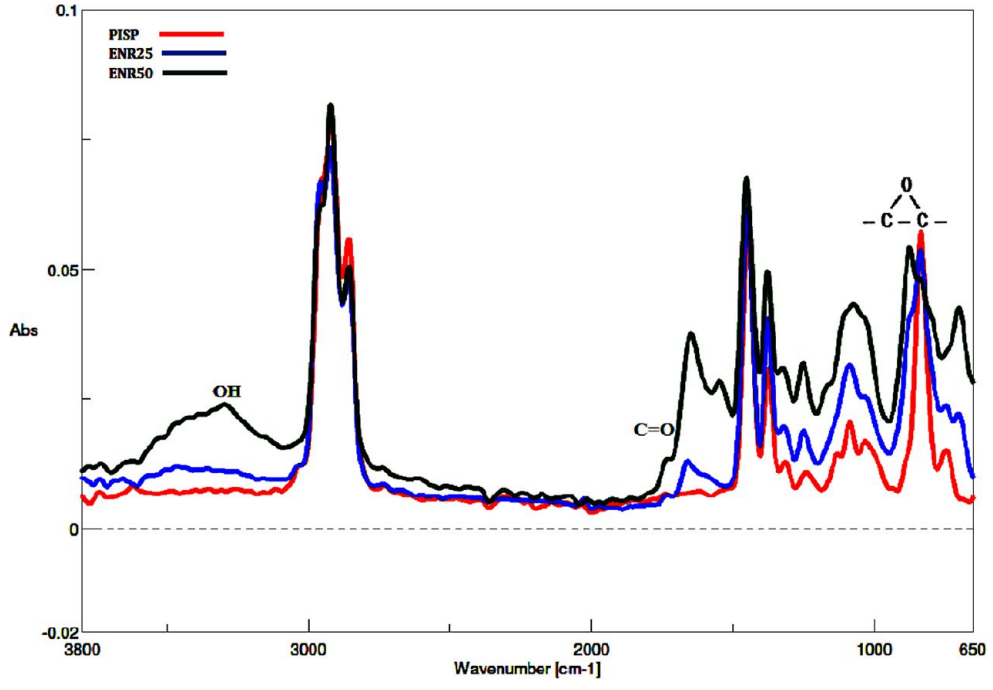

Figure 4. FTIR spectra of pure PISP, ENR25, and ENR50.

was left over the impact zones in each sample, which indicates a high temperature increase in the impact zone during the bullet impact when the bullet comes in contact with the sample at a high velocity (≤380 m/s). Such heating is the result of bullet friction and strain energy dissipation in the rubber.

Figure 6 shows the postimpact morphology of self-healed ENR50 sample as observed at SEM. An extensive recovery of the damage zone can be evidenced as indicated by the smooth outer surface at the impact zone. Moreover, the complete hole closure indicates a high level of interdiffusion at the damage

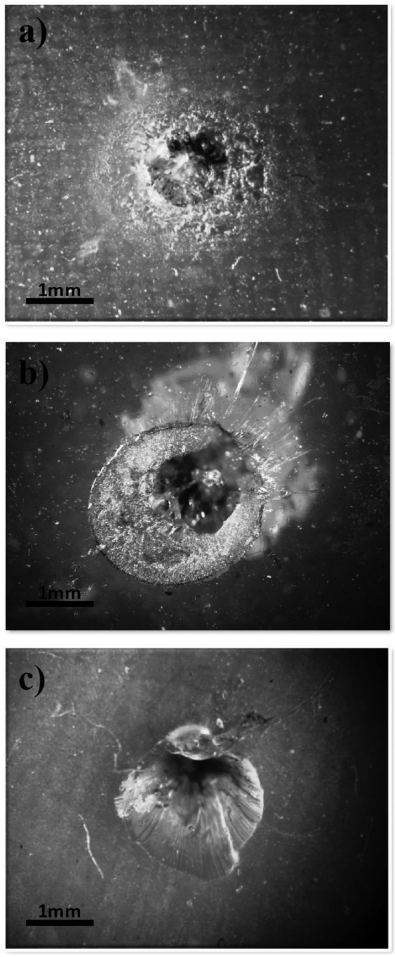

Figure 5. Optical images showing impact zones in vulcanized (0.5 wt % DCP) (a) ENR50, (b) ENR25, and (c) PISP.

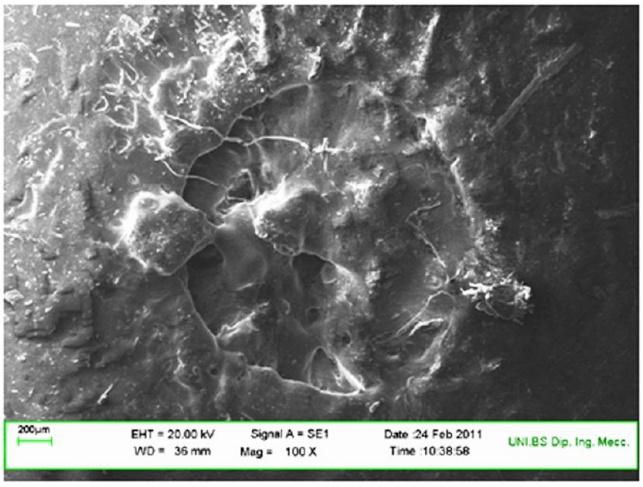

Figure 6. SEM image showing the bullet impact zone of ENR50 (vulcanized with 0.5 wt % DCP).

zone following the elastic recovery of high deformation imposed by the bullet. The elevated temperature at the impact zone should enhance the interdiffusion process because temperature has significant influence on the interdiffusion process of elastomer.[41] On the other hand, the T_g values reported in Table 2 would suggest a higher mobility for PISP and ENR25 but the open holes in ENR25 and PISP samples are clear indications of their healing failure following the ballistic damage. It is thus apparent that not only the mobility of macromolecular chains but also the level of epoxidation, along with the presence of epoxide ring-opened polar moieties, play significant role on the successful intermolecular diffusion and hole closure following the bullet impact.

Table 2. DSC Results of Pure and Vulcanized ENR50, PISP, and ENR50/PISP Blends

materials	T_g (°C)	
Pure PISP	−62	
Pure ENR25	−40	
Pure ENR50	−21	
ENR50 (0.5 DCP)	−20	
PISP (0.5 DCP)	−61	
ENR50/PISP (0.5 wt % DCP) (wt % PISP)	PISP phase	ENR50 phase
15	−61	−18
25	−60	−19
50	−61	−18

As in self-adhesion tests, a synergistic effect of interdiffusion and polar interactions (as evidenced in FTIR analysis) is expected to give a major contribution to the autonomic healing after bullet puncture. The puncture healing mechanism is, therefore, the result of an instantaneous elastic recovery, which brings the hole edges together, combined with rapid interdiffusion and intermolecular interactions among polar groups, which are made possible by the increased temperature.

Effect of Cross-Link Density on Self-Healing of ENR50. The above investigations concerned the self-healing behavior of slightly vulcanized (with 0.5 wt % DCP) ENR50 and ENR50/PISP blends. To understand the role of cross-link density, ENR50 was cross-linked with different amounts of DCP (0.2 to 3 wt %) and its self-healing behavior was investigated. Table 1 shows the results of pressurized air flow tests after bullet punctures, which confirm complete hole closure of ENR50 samples vulcanized with 0.2 to 0.8 wt % DCP. These samples showed efficient self-healing up to a pressure difference of 2 bar. In contrast, ENR50 vulcanized with 1 to 3 wt % DCP contents did not show full self-healing following the ballistic damage. As further evidence, Figure 7 shows the optical micrographs of the bullet impact zones in ENR50 samples with different DCP contents. It can be observed that complete hole closure can be achieved up to 0.8 wt % DCP content, whereas clear holes are observed in 2 and 3 wt % DCP vulcanized samples.

Figure 8 shows a plot of apparent cross-link density of ENR50 as a function of DCP content (wt%) measured by swelling tests. Cross-link density increases with increasing DCP content and above a certain cross-linking level no self-healing was observed. This suggests that as the cross-link density increases the self-healing ability decreases, probably because cross-linking hinders the polymer chain interdiffusion process, which is important for the self-healing of ballistic damages.

Effect of Blending ENR50 with PISP on Their Self-Healing. Blends of ENR50/PISP (vulcanized with 0.5 wt % DCP) were prepared to investigate the role of the epoxidation level (i.e., ENR50) and chain mobility (i.e., PISP) in the self-healing behavior following ballistic damage. The pressurized air flow test revealed that self-healing occurred in the blends containing 15 and 25 wt % PISP, whereas air tightness was not observed at the impact zone of sample containing 50 wt % PISP

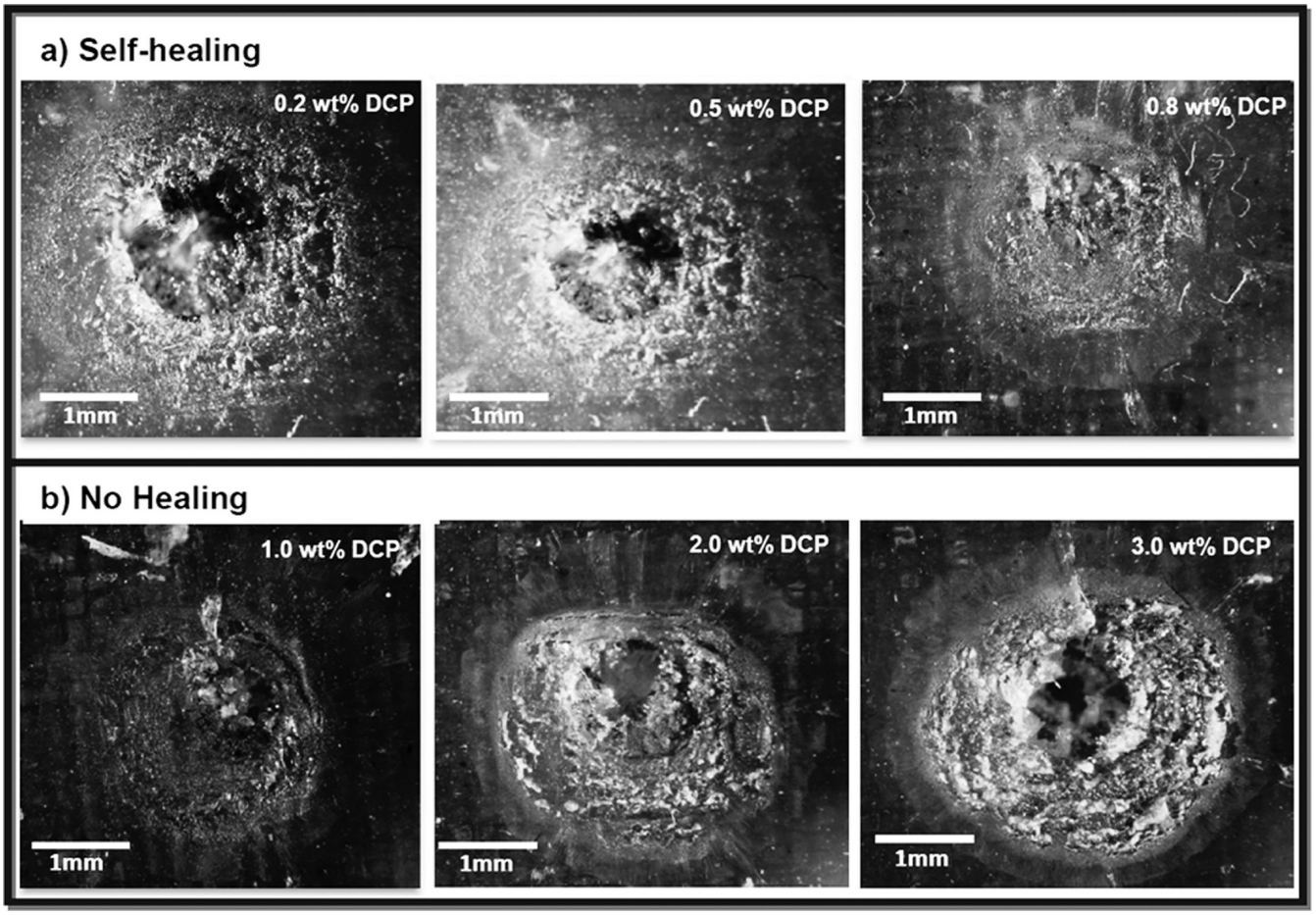

Figure 7. Optical Images Showing the Bullet Impact Zones in ENR50 Vulcanized with Different DCP Contents.

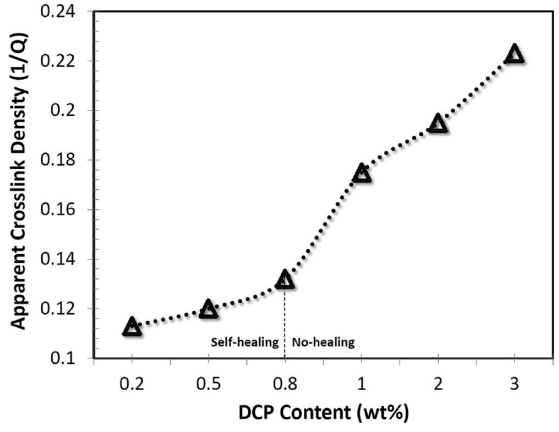

Figure 8. Apparent cross-link density of ENR50 as a function of DCP content.

(Table 1). In addition, higher self-healing efficiency was observed for the blend containing 15 wt % PISP.

Figure 9 shows the optical micrographs of the bullet impact zones in blend samples. A complete to partial hole closure can be observed in blends containing 85 and 75 wt % ENR50, respectively, whereas a clear hole can be noticed in the blends containing 50 wt % ENR50.

Figure 10 shows the TEM images of the unaffected areas in blend samples where the phase morphology can be detected. Inclusions of PISP having diameters ranging from 0.5 to 1.5 μm and 0.4 to 2.5 μm are distributed in a continuous ENR50 matrix of 15 and 25 wt % PISP blends, respectively. A remarkably different, cocontinuous morphology can be observed in the sample with 50 wt % PISP content.

The DSC study on the blends confirms the presence of a heterogeneous morphology as the T_g of both ENR50 and PISP phases could be detected (Table 2). It can be noticed that only the T_g of ENR50 phase is slightly affected in blends but almost constant value of T_g can be observed for PISP phase.

From the obtained results it can be inferred that the healing capacity of blends is significantly influenced by their composition. The higher self-healing efficiency in blend containing 15 wt % PISP compared to the lower mending ability in blend containing 25 wt % PISP clearly indicates that the amount of healing phase (i.e., ENR50) dominates the self-healing response. As observed in pure rubbers, it seems that when the average epoxidation level decreases below a critical value, the blend completely fails to heal the ballistic damage. At present, it is unclear if the blend morphology can also have a significant effect on the self-healing ability of blends.

CONCLUSIONS

The self-healing behavior of epoxidized natural rubber was investigated in two different test conditions. T-peel tests revealed a self-adhesion behavior of ENR50 which is responsible for healing the joint surfaces of ENR50 even at low temperatures. A higher level of epoxidation along with the presence of epoxide ring-opened polar groups enhanced self-adhesion assisted self-healing of rubbers.

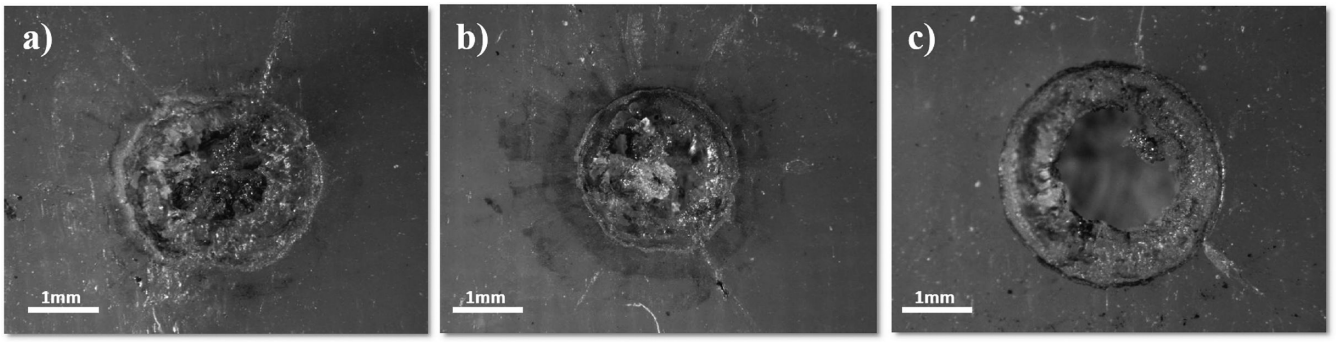

Figure 9. Optical images showing the bullet impact zones in ENR50/PISP blends (vulcanized with 0.5 wt % DCP): (a) 15, (b) 25, and (c) 50 wt % PISP-containing blends.

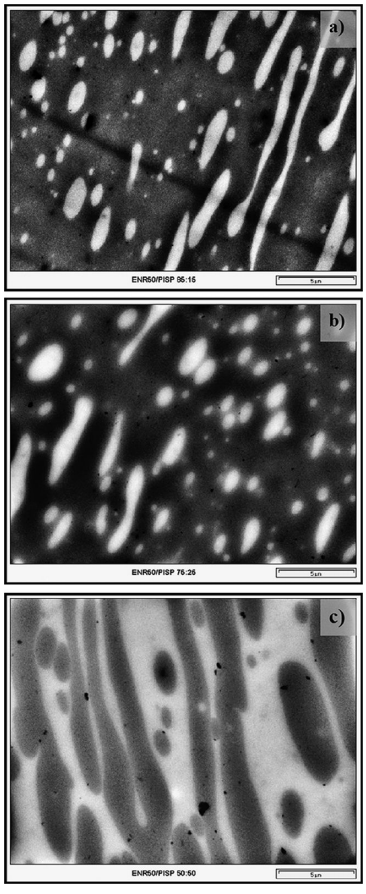

Figure 10. TEM images showing morphology of ENR50/PISP blends containing (a) 15, (b) 25, and (c) 50 wt % PISP.

Ballistic tests, can be considered as a self-healing study on shorter time scale in comparison with T-peel tests. They showed that also in this case, ENR with a higher epoxidation level was able to efficiently heal while no healing was observed in ENR25 and PISP. Moreover, self-healing in ENR50 was observed only at lower cross-link densities, thus indicating that self-healing in ENR50 is largely dependent on its structural property.

The results show that autohesion and self-healing are the result of molecular interdiffusion and effective polar interactions occurring when ENR50 surface are brought in contact. In the case of ENR25 and PISP, the lack of sufficient interdiffusion and absence of polar moieties do not allow a fast restoration of material cohesion.

Finally, it was shown that ENR50/PISP blends with sufficient amount of ENR50 can exhibit self-healing behavior following ballistic damage. However, further investigations are necessary to understand the role of morphology in blends.

AUTHOR INFORMATION

Corresponding Author

*E-mail: arifur.rahman@ing.unibs.it.

Notes

The authors declare no competing financial interest.

ACKNOWLEDGMENTS

The authors thank Dr. A. Callaioli for his assistance in TEM observations. The contributions of Mr. Bruno Romano of the Brescia Local Police Dept. in performing ballistic tests is also gratefully acknowledged. The technical assistance of Isabella Peroni and Gloria Spagnoli is also acknowledged.

REFERENCES

(1) Van Der Zwaag, S. An Introduction to Material Design Principles: Damage Prevention versus Damage Management. In *Self Healing Materials: An Alternative Approach to 20 Centuries of Materials Science*, 1st ed. ; Van Der Zwaag, S.; Springer: Amsterdam, The Netherlands, 2007; pp 1−18.

(2) Chen, X.; Dam, M. A.; Ono, K.; Mal, A.; Shen, H.; Nutt, S. R.; Sheran, K.; Wudl, F. A. *Science* **2002**, *295*, 1698−1702.

(3) Klukovich, H. M.; Kean, Z. S.; Iacono, S. T.; Craig, S. L. *J. Am. Chem. Soc.* **2011**, *133*, 17882−17888.

(4) Ghosh, B.; Urban, M. W. *Science* **2009**, *323*, 1458−1460.

(5) White, S. R.; Sottos, N. R.; Geubelle, P. H.; Moore, J. S.; Kessler, M. R.; Sriram, S. R.; Brown, E. N.; Viswanathan, S. *Nature* **2001**, *409*, 794−797.

(6) Mauldin, T. C.; Rule, J. D.; Sottos, N. R.; White, S. R.; Moore, J. S. *J. R. Soc. Interface.* **2007**, *4*, 389−393.

(7) Shchukin, D. G.; Zheludkevich, M.; Yasakau, K.; Lamaka, S.; Ferreira, M. G.; Möhwald, H. *Adv. Mater.* **2006**, *18* (13), 1672−1678.

(8) Andreeva, D. V.; Fix, D.; Shchukin, D. G. *Adv. Mater.* **2008**, *20* (14), 2789−2794.

(9) Andreeva, D. V.; Shchukin, D. G. *Mater. Today* **2008**, *11* (10), 24−30.

(10) Wietor, J. L.; Sijbesma, R. P. *Angew. Chem., Int. Ed.* **2008**, *47*, 8161−8163.

(11) Burattini, S.; Greenland, B. W.; Merino, D. H.; Weng, W.; Seppala, J.; Colquhoun, H. M.; Hayes, H.; Mackey, M. E.; Hamley, I. W.; Rowan, S. J. *J. Am. Chem. Soc.* **2010**, *132*, 12051−12058.

(12) Cordier, P.; Tournilhac, F.; Soulié-Ziakovic, C.; Leibler, L. *Nature* **2008**, *451*, 977−980.

(13) Ciferri, A. *Chem.—Eur. J.* **2009**, *15*, 6920−6925.

(14) Maes, F.; Montarnal, D.; Cantournet, S.; Tournilhac, F.; Corté, L.; Leibler, L. *Soft Matter* **2012**, *8* (5), 1681−1687.

(15) Chen, Y.; Kushner, M. A.; Williams, A. G.; Guan, Z. *Nat. Chem.* **2012**, *4*, 467−472.
(16) Zheng, P.; McCarthy, T. J. *J. Am. Chem. Soc.* **2012**, *134*, 2024−2027.
(17) Press release, 05/27/2009. Self-healing elastomer enters industrial production. (http://www.arkema.com/group/en/press/)
(18) Bac, N. V.; Huu, C. C. *J. Macromol. Sci., Part A: Pure Appl. Chem.* **1996**, *33* (12), 1949−1955.
(19) Garcia, S. J.; Fischer, H. R.; van Der Zwaag, S. *Prog. Org. Coat.* **2011**, *72* (3), 211−221.
(20) Bergman, S. D.; Wudl, F. *J. Mater. Chem.* **2007**, *18* (1), 41−62.
(21) Pummere, R.; Burkard, P. A. *Uber Kautchuk. Ber. Dtsch. Chem. Ges.* **1922**, *55*, 3458.
(22) Netherlands Patent Application 6 413 160, 1965.
(23) British Patent 1 083 316, 1967.
(24) Gelling, I. R.; Porte, M. In *Natural Rubber Science and Technology*; Robberts, A. D., Ed.; Oxford University Press: Oxford, U.K., 1990; Chapter 10.
(25) Gelling, I. R.; Tinker, A. J.; Rahman., H. A. *J. Nat. Rubber Res.* **1991**, *6*, 1.
(26) Johnson, T.; Thomas, S. *Polymer* **1999**, *40*, 3223−8.
(27) Hashim, A. S.; Kohjiya, S. *Kautsch. Gummi Kunstst.* **1993**, *46*, 208−13.
(28) Bibi, A. N.; Boscott, D. A.; Butt, T.; Lehrle, R. S. *Eur. Polym. J.* **1988**, *24*, 1127−31.
(29) Koklas, S. N.; Sotiropoulou, D. D.; Kallitsis, J. K.; Kalfoglou, N. K. *Polymer* **1991**, *32*, 66−72.
(30) Davies, C. K. L.; Wolfe, S. V.; Gelling, I. R.; Thomas, A. G. *Polymer* **1983**, *24*, 107−13.
(31) Rahman, M. A.; Penco, M.; Peroni, I.; Ramorino, G.; Janszen, G.; Landro, Di.L. *Smart Mater. Struct.* **2012**, *21*, 035014.
(32) Rahman, M. A.; Penco, M.; Peroni, I.; Ramorino, G.; Grande, M. A.; Landro Di, L. *ACS Appl. Mater. Interfaces* **2011**, *3*, 4865−4874.
(33) Kurata, M.; Tsunashima, Y.; Iwama, Kamada, M. Viscosity-Molecular Weight Relationships and Unperturbed Dimensions of Linear Chain Molecules. In *Polymer Handbook*, 4th ed.; Brandrup, J., Immergut, E.H., Grulke, E.A., Eds.; Wiley: New York,1998; pp IV1−IV60.
(34) Choi, S. S.; Kim, J. C.; Ko, J. E.; Cho, Y. S.; Shin, W. G. *J. Ind. Eng. Chem.* **2007**, *13*, 1017−1022.
(35) Voyutskii, S. S.; Margolina, Y. I. *Uspek. Khim.* **1949**, *18*, 449−461.
(36) Duncan, B C.; Abbott, S G.; Roberts, R A. *Measurement Good Practice Guide No. 26: Adhesive Tack*; NPL Doc. PDB: 2294 ; National Physical Laboratory: Teddington, U.K., 1999.
(37) Thitithammawong, A.; Nakason, C.; Sahakaro, K.; Noordermeer, J. W. M. *Eur. Polym. J.* **2007**, *43*, 4008−4018.
(38) Fetters, L. J.; Lohse, D. J.; Milner, S. T.; Graessley, W. W. *Macromolecules* **1999**, *32*, 6847−6851.
(39) Gelling, I. R. *Rubber Chem. Technol.* **1985**, *58*, 86−96.
(40) Ng, S. C.; Gan, L. H. *Eur. Polym. J.* **1981**, *17*, 1073−1077.
(41) Ansarifar, M. A. Adhesion of Elastomers. In *Mechanical Properties and Testing of Polymers*; Swallowe, G.M., Ed.; Kluwer Academic Publishers: Dordrecht, The Netherlands, 1999; p 5.